Detecting igneous rocks in the pre-salt with elastic FWI

Gabriel Pacheco, Ana Araújo, Diego Costa, Karine Pereira, Luis Cypriano (Viridien)*

Summary

Brazilian pre-salt often exhibits geologically complex settings with many challenges for oil and gas exploration and production. One of these key challenges is the presence of igneous rocks. We analyze the ability of full-waveform inversion (FWI) to identify and detect this class of rock using an OBN data set from the Santos Basin. Comparisons between acoustic and elastic FWI are studied. Thanks to the improved physics, elastic FWI shows more accurate representations of the distribution and plumbing systems of igneous rocks in the pre-salt. Moreover, the resulting FWI Images show uplift over the classical reverse-time migration (RTM) images that have historically been used to image the field.

Introduction

Seismic acquisition and imaging have significantly evolved over the past decade. Ocean-bottom-node (OBN) data have provided a step-change in quality, as the improved signal-to-noise ratio (S/N) in the low-frequency range, long offsets, and full-azimuthal coverage are essential ingredients for better seismic imaging. The combination of advanced model building and imaging algorithms, such as Time-Lag FWI (TLFWI, Zhang et al., 2018) and Least-Squares RTM (LSRTM, Wang et al., 2016), have helped overcome many imaging challenges (Liu et al., 2019). More recently, FWI Imaging (Zhang et al., 2020) has emerged. While LSRTM relies on the Born approximation and does not account for non-linear propagation effects, FWI Imaging – utilizing more accurate physics – considers the full-wavefield propagation and provides better illumination, resolution, and S/N. Complex geologies with complicated scattering bodies benefit the most from this approach (Zhang et al., 2020).

The advantages of producing high-frequency FWI models and images extend beyond structural imaging. The high-frequency velocity model itself can provide relevant information that aids in a better understanding of the geology. Elastic FWI is best suited for such purposes (Brando et al., 2023), since in the presence of large impedance contrasts, such as salt-sediment interfaces and igneous bodies, elastic effects are expected. In this case, the use of an elastic propagation engine results in a more accurate inversion (Wu et al., 2022). Hence, the application of high-frequency FWI and FWI Imaging provides an attractive opportunity for Brazilian pre-salt reservoirs.

Brazilian pre-salt reservoirs often exhibit complex geologies and petrophysics. The presence of intrusive swarming and volcanism can exert considerable influence on the basin

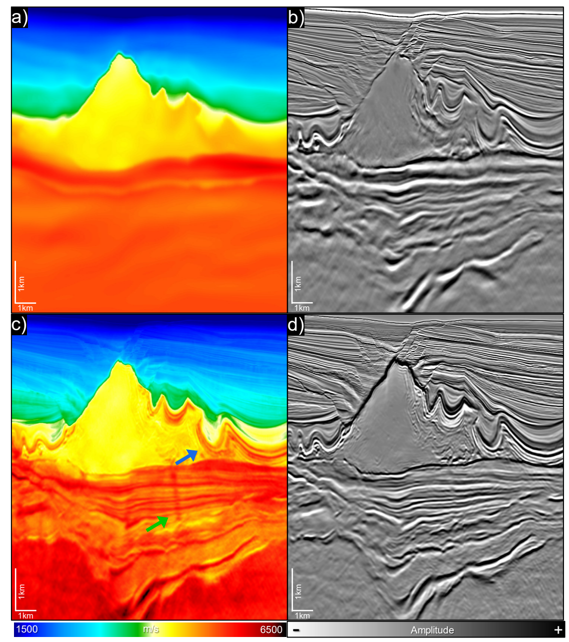

Figure 1 : Legacy velocity model (a), Legacy 45 Hz RTM (b), 30 Hz AFWI velocity model (c), and 30 Hz AFWI Image (d). The blue arrow points to an overhang, reshaped by AFWI. The green arrow points to a vertical anomaly that might indicate a feeder dyke.

geodynamics and its petroleum systems. These magmatic pulses introduce diverse risks, including reservoir compartmentalization, CO_2 contamination, and ultimately impacts hydrocarbon exploration and production (Planke et al., 2005; Senger et al., 2017). A better understanding of these systems through seismic data is critical to reducing uncertainty when planning exploration and development work in the field. We demonstrate how high-frequency FWI could help achieve this objective: specifically, FWI Images produce clearer pre-salt images when compared to the classical RTM approach, and the FWI velocity model itself can be used to map the igneous system. It is shown that elastic FWI can provide a more accurate representation of the system. All of this together promotes a deeper geological understanding of the area.

Method

The study area is covered by an OBN seismic data set with a maximum offset of 20 km. A legacy processing flow was carried out in 2021, and its velocity model and seismic (45 Hz RTM) are used as references. Before starting inversions, the legacy model was smoothed to remove any imprint of

10.1190/image2024-4099750.1

manual interpretation. Additionally, well-tie tomography was applied to obtain reasonable anisotropy models for input to FWI. Acoustic FWI (AFWI) and elastic FWI (EFWI) inversions were run up to 30 Hz. Both tests employed the time-lag cost function, which has consistently proven to be robust against cycle-skipping, as well as being less sensitive to amplitude discrepancies (Zhang et al., 2018). Note that in both AFWI and EFWI, only the P-wave velocity is inverted, with EFWI preserving a fixed V_S/V_P input relation in the wavefield propagation.

Results

A comparison between the legacy and 30 Hz AFWI velocities and images is presented in Figure 1. The legacy model (Figure 1a) is considerably smooth, with few noticeable contrasts. The 30 Hz AFWI (Figure 1c) added many details to the model. The sediment layers are better defined, the top of salt is reshaped, especially around overhangs (blue arrow in Figure 1c), and different layers are revealed in the pre-salt. Furthermore, high-frequency AFWI can capture many vertical anomalies that could not be imaged in the seismic. The green arrow in Figure 1c points to a vertical anomaly that may indicate a feeder dyke. The AFWI Image (Figure 1d) also exhibits significant improvements compared to the legacy RTM (Figure 1b), enhancing pre-salt faults and providing better definition of the base of salt and the basement. Additionally, pre-salt events are more continuous after FWI, as it also compensates for illumination issues.

The acoustic approximation loses accuracy in the presence of strong impedance contrasts. In the study area, the AFWI velocity fails to accurately capture the velocity of the igneous rocks crossing the reservoir level. For example, Figure 2 shows a comparison between AFWI and EFWI overlayed with a well sonic log. The yellow arrow points to the depth where the igneous rock occurs, which is better captured by EFWI compared to AFWI.

An overall comparison of the legacy, AFWI, and EFWI results is shown in Figure 3. Between the legacy and AFWI, the same observations mentioned earlier can be emphasized. The high-resolution AFWI enhances the velocity by capturing details in the subsurface (Figures 3a and 3c). In the image domain, AFWI Imaging brings continuity and resolution to the pre-salt events (Figures 3b and 3d). Compared to AFWI, EFWI yields a sharper velocity (Figure 3e) with stronger contrasts in the pre-salt. EFWI Imaging exhibits slight uplifts compared to AFWI Imaging, with a sharper top of salt event and reduced halo, and slightly better illuminated pre-salt (Figures 3d and 3f). Furthermore, the enhanced accuracy of the EFWI velocity model provides extra information for identifying igneous and other pre-salt rocks, such as those represented by low-velocity anomalies.

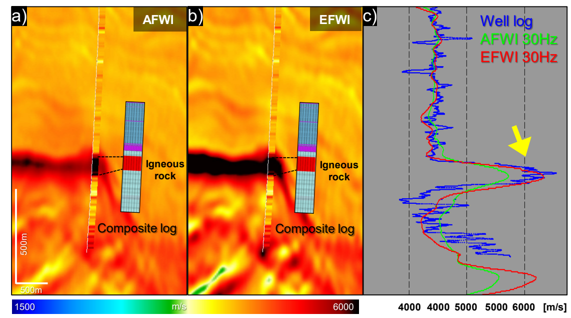

Figure 2: 30 Hz AFWI (a), 30 Hz EFWI (b), and well sonic log comparison (c).

The geological features captured by EFWI were also captured by AFWI; however, these features are further enhanced in the former. Figure 4 shows a second comparison among the legacy, AFWI, and EFWI results. The black arrow highlights a high-velocity anomaly shaped as a hydrothermal vent, while the structure indicated by the green arrow suggests a strata-discordant sill feeding the vent and compartmentalizing the reservoir. Both features appear to be better captured by EFWI.

Igneous rock distribution

Understanding the presence and distribution of igneous rocks is key to evaluating the reservoir. To better explore this aspect, a velocity filtering study is proposed. Initially, we extract the lithological intervals from igneous rocks present in the reservoir from a set of wells. Velocities of these igneous bodies are then extracted from the sonic logs to obtain a representative average velocity. The analysis revealed that a minimum cut-off velocity of 5509 m/s is representative for igneous rocks within the reservoir.

Figure 5 represents a well that sampled three intercalations of magmatic origin, limited by the markers TI and BI (top and base of igneous). To better represent the layers and not the interface, a -90° phase rotation was applied to the FWI Images in this display. At first glance, one may notice that the FWI models (Figures 5a and 5e) in the interval limited by TR (top of reservoir) and BR (base) indicate a wide range of velocities, revealing a complex and heterogenous target, where the EFWI response offers more delineation and sharper contrasts than the AFWI. When filtering the velocities with the igneous filter in Figures 5b and 5f, it is noticeable that the amplitude differences between the FWI Images are subtle, but those between the velocity models are not. When zooming in (Figures 5d and 5h), EFWI offers a better match with well markers, showing that what once was an isolated sill in the AFWI is now better interpreted as a multi-level sill compound. It exhibits junctions by the tips and the confinement of one against the other (Hansen et al., 2004).

10.1190/image2024-4099750.1

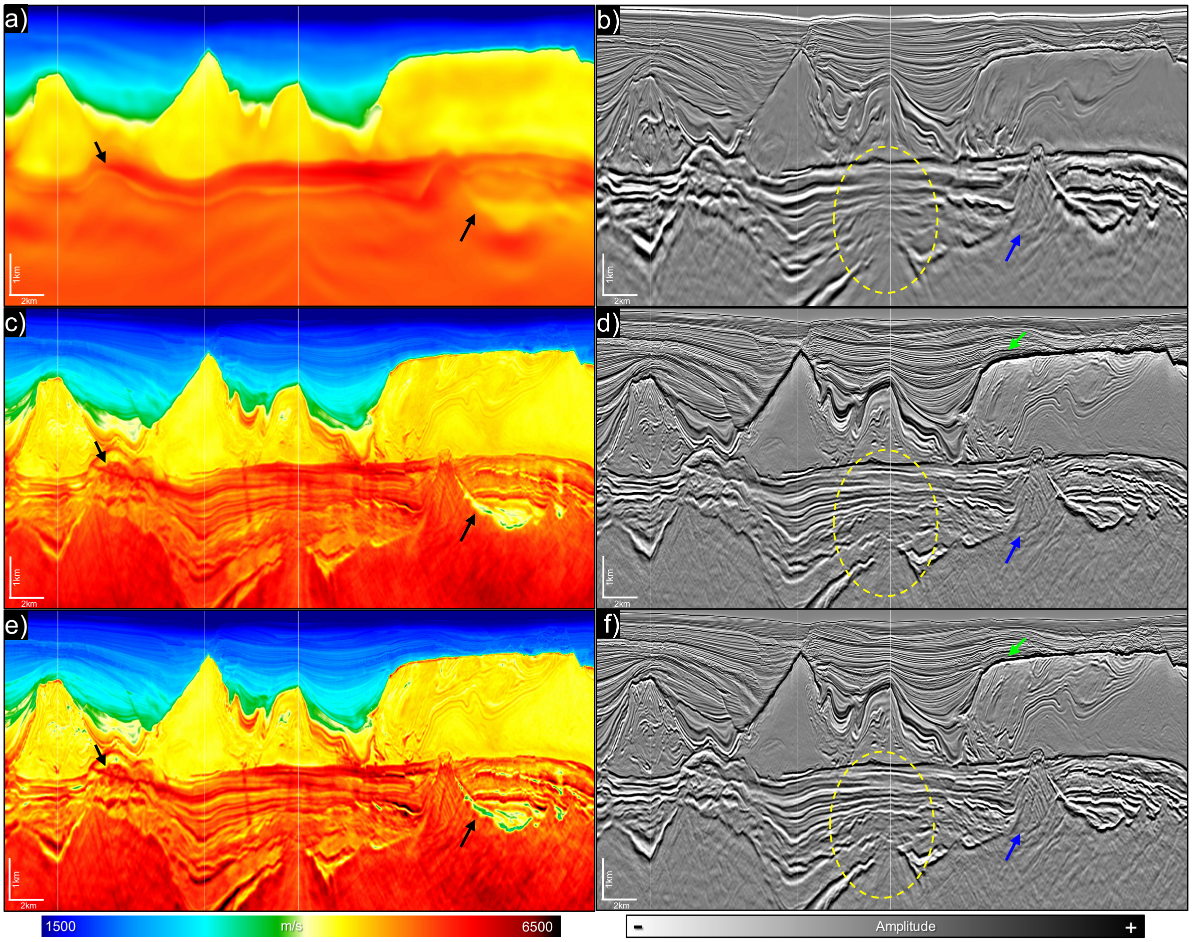

Figure 3: Legacy velocity model (a), Legacy 45 Hz RTM (b), 30 Hz AFWI velocity model (c), 30 Hz AFWI Image (d), 30 Hz EFWI velocity model (e), and 30 Hz EFWI Image (f). The black arrows indicate the details on the velocity model captured by AFWI and enhanced by EFWI compared to the legacy model. On the images, the yellow dashed area shows a region of impact of FWI Imaging compared to the legacy RTM. The green arrow highlights the sharper top of salt on the EFWI Image, and the blue arrow indicates better defined faults on the basement.

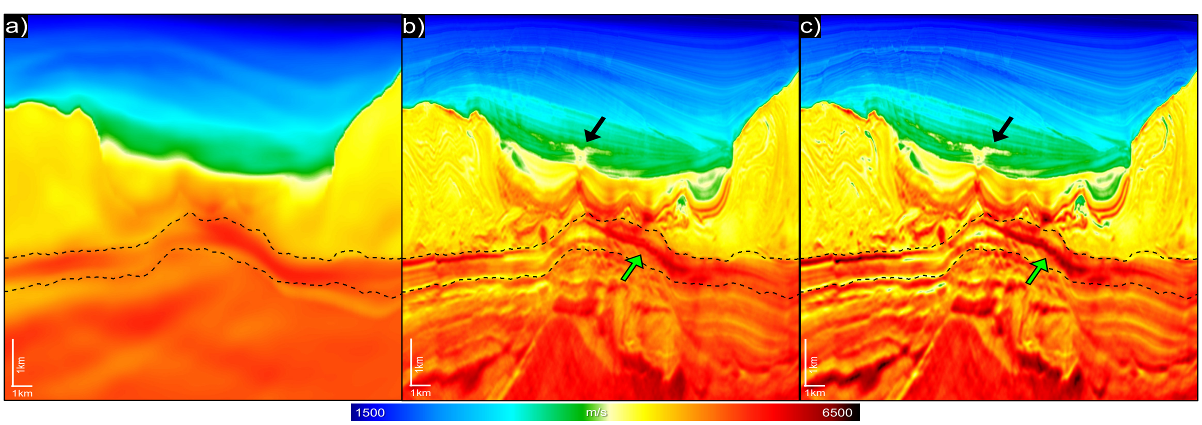

Figure 4: Legacy velocity model (a), 30 Hz AFWI velocity model (b), and 30 Hz EFWI velocity model (c). The dashed black lines represent top and base of the reservoir. The black arrow highlights a high-velocity anomaly shaped as a hydrothermal vent, and the green arrow points to a strata-discordant sill feeding the vent and compartmentalizing the reservoir.

The maps of the IR1 and IR2 (intra-reservoir) horizons show the filtered velocities in the study area. It is observed that rounded shapes (green arrows), typical of saucer-shaped sills, are more continuous and better represented in the EFWI. Similarly, straight features (yellow arrow), typical of dykes that use fractures during emplacement, are more distinctly delineated in the elastic when compared to the acoustic. In the AFWI, there is only a small indicator, while in the EFWI, a trend is observed. Numbered arrows (1) and (2) demonstrate the main differences at the well location. AFWI does not seem sensitive to the applied cut-off near the top of the reservoir, while EFWI is. In the case of arrow (2), it is noticeable that AFWI implies the possibility of a circular closure, but EFWI suggests that there is a 4-way closure affecting reservoir connectivity.

Conclusions

FWI Imaging results show improvements in pre-salt imaging definition and resolution when compared with legacy RTM images. A high-frequency AFWI velocity model revealed geological features, which might be associated with dykes and conduits. However, we show that EFWI better captures these details, helping to reduce exploratory uncertainties, especially related with igneous rock identification. Finally, we highlight that enhancing the quality of velocity models is a continual process and, for example, the model could benefit from technologies such as multiparameter elastic FWI, as well as even higher frequency inversions.

Acknowledgments

We thank CGG and Petrobras for the permission to publish this work.

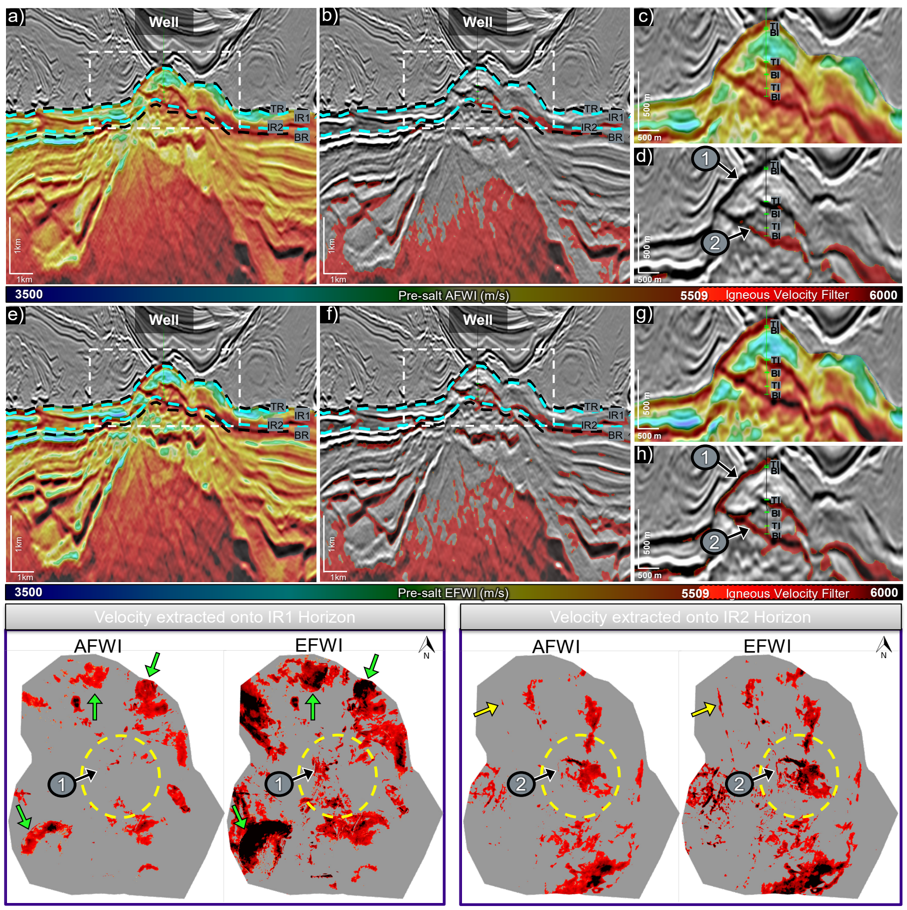

Figure 5: Igneous velocity filtering at a given well location (yellow circle in the maps). In (a) and (e) pre-salt AFWI and EFWI, respectively. In (b) and (f) the filtered AFWI and EFWI models from 5509 m/s. Dashed white square indicates the zoomed area in (c), (g) with the pre-salt velocity overlaid and (d) and (h) with the filtered velocities. Arrows (1) and (2) indicate differences between AFWI and EFWI response. Maps on the bottom display the velocities extraction at the two horizons. Green arrows indicate rounded velocity anomalies, while yellow arrows show straight-oriented anomalies.

REFERENCES

Brando, G., B. Huard, and L. Cypriano, 2023, Imaging the pre-salt with elastic FWI using OBN data: Third International Meeting for Applied Geoscience & Energy, SEG/AAPG, Expanded Abstracts, 685–689, doi: https://doi.org/10.1190/image2023-3917169.1.

Hansen, D. M., J. A. Cartwright, and D. Thomas, 2004, 3D seismic analysis of the geometry of igneous sills and sill junction relationships, *in* R.J. Davies, J.A. Cartwright, S.A. Stewart, M. Lappin, and J.R. Underhill, eds., 3D Seismic Technology: Application to the Exploration of Sedimentary Basins: Geological Society of London Memoir **29**, 199–208, https://doi.org/10.1144/GSL.MEM.2004.029.01.19.

Liu, Y., Y. Chen, H. Ma, C. Peng, G. Mohapatra, W. Martins, G. Duncan, and S. Checkles, 2019, Least-squares RTM with ocean bottom nodes: Potentials and challenges: 89th Annual International Meeting, SEG, Expanded Abstracts, 4241–4245, doi:https://doi.org/ 10.1190/segam2019-3216736.1.

Planke, S., T. Rasmussen, S. S. Rey, and R. Myklebust, 2005, Seismic characteristics and distribution of volcanic intrusions and hydrothermal vent complexes in the Vøring and Møre basins, *in* A.G. Doré, and B.A. Vining, eds., Petroleum Geology: North-West Europe and Global Perspectives: Geological Society of London Proceedings of the 6th Petroleum Geology Conference, 833–844, doi: https://doi.org/10.1144/0060833.

Senger, K., J. Millett, S. Planke, K. Ogata, C.H. Eide, M. Festøy, O. Galland, and D.A. Jerram, 2017, Effects of igneous intrusions on the petroleum system: A review: First Break, **35**(6), 47–56, doi: https://doi.org/10.3997/1365-2397.2017011.

Wang, P., A. Gomes, Z. Zhang, and M. Wang, 2016, Least-squares RTM: Reality and possibilities for subsalt imaging: 86th Annual International Meeting, SEG, Expanded Abstracts, 4204–4209, doi: https://doi.org/10.1190/segam2016-13867926.1.

Wu, Z., Z. Wei, Z. Zhang, J. Mei, R. Huang, and P. Wang, 2022, Elastic FWI for large impedance contrasts: 2nd International Meeting for Applied Geoscience & Energy, SEG, Expanded Abstracts, 3686–3690, doi: https://doi.org/10.1190/image2022-w17-02.1.

Zhang, Z., J. Mei, F. Lin, R. Huang, and P. Wang, 2018, Correcting for salt misinterpretation with full-waveform inversion: 88th Annual International Meeting, SEG, Expanded Abstracts, 1143–1147, doi: https://doi.org/10.1190/segam2018-2997711.1.

Zhang, Z., Z. Wu, Z. Wei, J. Mei, and R. Huang, 2020, FWI Imaging: Full-wavefield imaging through full waveform inversion: 90th Annual International Meeting, SEG, Expanded Abstracts, 656–660, doi: https://doi.org/10.1190/segam2020-3427858.1.